Biomaterials 29 (2008) 3720–3728

Contents lists available at ScienceDirect

Biomaterials

journal homepage: www.elsevier.com/locate/biomaterials

Nanofibrous polyhydroxyalkanoate matrices as cell growth supporting materials

Xiao-Tao Li [a,1], Yan Zhang [a,1], Guo-Qiang Chen [a,b,*]

[a] Multidisciplinary Research Center, Shantou University, Shantou 515063, Guangdong, China
[b] Department of Biological Sciences and Biotechnology, Tsinghua University, Beijng 100084, China

ARTICLE INFO

Article history:
Received 6 March 2008
Accepted 7 June 2008
Available online 27 June 2008

Keywords:
PHB
Polyhydroxybutyrate
Nanofiber
Matrix
HaCat cells
Biocompatibility
Tissue engineering

ABSTRACT

Polyhydroxyalkanoates (PHAs) have been demonstrated to be a family of biopolymers with good biodegradability and biocompatibility. To mimic the real microenvironment of extracellular matrix (ECM) for cell growth, novel nanofiber matrices based on PHA polymers were prepared via a phase separation process. Three-dimensional interconnected fibrous networks were observed in these matrices with average fiber diameters of 50–500 nm, which are very similar to the major ECM component collagen. Compared with nanofiber matrix made of poly(L-lactide), the mechanical properties of PHA nanofiber matrices were significantly improved, especially those matrices of PHA blends PHB/PHBHHx containing polyhydroxybutyrate (PHB) and copolyesters PHBHHx consisting of 3-hydroxybutyrate and 3-hydroxyhexanoate, and PHB/P3HB4HB that are PHB blended with copolyesters of 3-hydroxybutyrate and 4-hydroxybutyrate, respectively. More importantly, cell attachment and growth of human keratinocyte cell line HaCat on the nanofiber PHA matrices showed a notable improvement over those on PHA matrices prepared via an ordinary solution casting method. It was therefore proposed that PHA nanofiber matrices combined the advantages of biodegradation, improved mechanical strengths and the nanostructure of a natural extracellular matrix, leading to a better cell compatibility, thus they can be used for future implant biomaterial development.

1. Introduction

Polyhydroxyalkanoates (PHAs) is a family of biopolyesters produced by many microorganisms [1]; they have been widely investigated for applications as tissue engineering materials [2,3]. Poly(R-3-hydroxybutyrate) (PHB) with a high crystallinity is one of the most well characterized homopolymer [4,5]. PHB has been investigated for uses as surgical suture [6], nerve repair [7], drug-delivery systems [8] and soft tissue repair [9]. Recently, the TephaFLEX® absorbable suture based on poly(R-4-hydroxybutyrate) launched by US company Tepha has been approved by the US Food and Drug Administration (FDA) for clinical applications. To overcome the brittleness and the narrow processing window of PHB [10–12], copolymers of R-3-hydroxybutyrate and R-3-hydroxyvalerate, abbreviated as PHBV, and poly(R-3-hydroxybutyrate-*co*-R-3-hydroxyhexanoate) (PHBHHx) as well as poly(R-3-hydroxybutyrate-*co*-R-4-hydroxybutyrate), abbreviated as P3HB4HB, were produced [13]. These PHAs have shown good biodegradability and biocompatibility with improved mechanical properties over PHB [2,3,14]. PHB blended with PHBHHx or P3HB4HB had demonstrated improved properties for potential applications in tissue engineering [15,16].

On the other hand, a lot of interests have been paid to mimic the characteristics of natural extracellular matrix (ECM) to facilitate cell seeding, adhesion, proliferation, differentiation and neo tissue genesis [17]. Various matrices prepared using many different methods including particulate leaching [18], textile technologies [19] and phase separation [20,21]. Although these artificial matrices showed certain advantages, the diameters of the matrix fibers and pores were often at micron sizes and still far from the natural nanoscale extracellular matrix (ECM) [22,23]. For example, collagen I, a major natural extracellular matrix and primary component of dermal, is a three-dimensional network structure composed of natural fibers ranging from 50 to 500 nm [24,25]. Zhang et al. had created self-assembled nanofibers with a diameter of 10–20 nm using ionic self-complementary oligopeptides [26]. These self-assembling oligopeptides can be fabricated into nanofiber scaffolds for three-dimensional culture of mammalian cells including osteoblasts, hippocampal neurons and adult mouse neural stem cells [27–29]. Ma et al. achieved to prepare nanoscale fibrous ECM using poly(L-lactide) (PLLA) [30], and PLLA fibrous scaffolds used for bone regeneration engineering had shown to be efficient [17,31]. Hence, the design of nanofeatured scaffolds has become one of the exciting new areas in the tissue engineering.

* Corresponding author. Multidisciplinary Research Center, Shantou University, Shantou 515063, Guangdong, China. Tel.: +86 754 82901186; fax: +86 754 82901175.
E-mail address: chengq@stu.edu.cn (G.-Q. Chen).
[1] Both authors contributed equally to this research.

0142-9612/$ – see front matter © 2008 Published by Elsevier Ltd.
doi:10.1016/j.biomaterials.2008.06.004

In this study, for the first time, we attempted to fabricate PHA nanofiber matrices combining the advantages of natural biodegradable polymers and the nanostructure of natural extracellular matrix. The cell growth supporting ability of these nanofiber matrices was studied.

2. Materials and methods

2.1. Materials

Poly(R-3-hydroxybutyrate) (PHB, Mw: 504 kDa) was purchased from Nantian Co. Ltd., Jiangsu, China. Poly(3-hydroxybutyrate-*co*-3-hydroxyhexanoate) (PHBHHx) containing 12 mol% 3-hydroxyhexanoate (3HHx) with a Mw of 270 kDa and poly-(3-hydroxybutyrate-*co*-4-hydroxybutyrate) [P(3HB-4HB)] containing 12 mol% 4-hydroxybutyrate (4HB) with a Mw of 540 kDa were kindly donated from Microbiology Laboratory, Tsinghua University, Beijing in China. All other chemicals were analytical reagents.

2.2. Fabrication of PHA matrices

PHB was dissolved in chloroform at 60 °C to become a clear solution; 1.0–6.0 mL dioxane was added in the 50 mL beaker with 10 mL PHB chloroform solution. The mixture was incubated in the frig (4 °C) for a sufficient time to allow gel formations in the beaker. The gels were immersed into water for 1 day with twice replacements of the distilled water. Subsequently, the gels were placed in a freeze-dryer (Modulyo D-230, Thermo, USA) for 48 h after 1 h incubation at −80 °C. On the other hand, some PHB solutions added with dioxane were incubated in liquid nitrogen for 15 min, or sonicated for 20 min before the gel formation process. The PHB blended with different amounts of PHBHHx or P3HB4HB was treated with the above mentioned procedure to prepare for the PHA nanofiber matrices.

For a comparison of cell growth behavior, ordinary solid-walled matrices and unique nanofibrous matrices made of various PHAs were prepared. The preparation process of solid-walled matrices was described previously [15,38]. Briefly, 1.0 g of PHB, PHB/PHBHHx (70:30) or PHB/P3HB4HB (70:30) material was dissolved in 50 mL of chloroform at 60 °C. The solution was poured into 120-mm Petri dishes. The dishes were then maintained at room temperature to allow evaporation of chloroform for 1 day. Subsequently, the dishes with casting matrices were placed in a freeze-dryer (Modulyo D-230, Thermo, USA) for 48 h. The evaporation of solvent resulted in the formation of solid-walled matrices with approximately 200 μm in thickness measured by Vernier caliper and SEM. Prior to application in cell cultures, all resulting matrices including solid-walled and nanofibrous matrices were cut uniformly into disks of 1.5 cm in diameter and sterilized by immersion in 75% (v/v) ethanol for 2 h and ultraviolet radiation for 1 h. Then, all matrices were immersed in PBS overnight.

2.3. Characterization

2.3.1. Scanning electron microscopic (SEM) studies

The PHA matrices were mounted on aluminum stumps, followed by coating with gold in a sputtering device for 1.5 min at 15 mA. They were then examined under a scanning electron microscope (SEM, JSM-6360LA, Japan).

2.3.2. Wide-angle X-ray diffraction (WAXD) studies

Wide-angle X-ray diffraction (WAXD) of the polyester samples was conducted using an X-ray powder diffractometer (D8 Advance, Bruker, Germany). Cu Kα radiation ($\lambda = 0.1541$ nm) was used as the source, and the X-ray diffraction patterns were recorded in the range $2\theta = 10°$–$50°$. The percentage of crystallinity was calculated from diffracted intensity according to Vonk's method [32].

2.3.3. Study on the density of fibrous matrices

The estimated densities and porosities of the fibrous matrices were obtained as follows: the circular discs of the fibrous matrices were fabricated as described in Section 2.2. The diameter and height of a disc were measured to calculate the volume. The weight of the specimen was measured with an analytical balance accurate to 10^{-4} g. The density was calculated from the volume and weight. The porosity ε was calculated from the measured overall densities D_f of the fibrous matrix and the skeletal density D_p:

$$\varepsilon = \frac{D_p - D_f}{D_p} \tag{1}$$

For the fibrous matrix, the skeletal density was the density of the polymer, which was given by

$$D_p = \frac{1}{\frac{1 - X_c}{D_a} + \frac{X_c}{D_c}} \tag{2}$$

where X_c is the degree of crystallinity of a polymer. For PHB, $D_a = 1.177$ g/mL (density of amorphous polymer) and $D_c = 1.260$ g/mL (density of 100% crystalline polymer) [33]. Also, in the blended matrices of PHB/PHBHHx or PHB/P3HB4HB, $D_c = 1.260$ g/mL, which was due to the crystallinity attributed from R-3-hydroxybutyrate (3HB) [15,16]; and the $D_a = 1.177$ g/mL, because 3HB sustains the main content of these matrices and the amorphous density resulted from small amounts of 3HHx or 4HB is also approximately equal to 1.177 g/mL [16,38].

2.3.4. Study on average nanofiber diameters

An average nanofiber diameter was calculated from the SEM images. Eighty fibers were measured for each sample. A surface area-to-volume ratio was estimated based on the average fiber diameter. The surface areas of the fiber ends were neglected based on a very large aspect ratio of the fibers, virtually a continuous fiber network (Scheme 1), so that the surface area of a fiber was calculated with the equation:

$$A_f = \pi \cdot d \cdot l \tag{3}$$

where d is the diameter of the fiber and l the length of the fiber. The volume of a fiber is given by

$$V_f = \frac{\pi \cdot d^2 \cdot l}{4} \tag{4}$$

Therefore, the surface-to-volume ratio is given by

$$\frac{A_f}{V_f} = \frac{\pi \cdot d \cdot l}{\frac{\pi \cdot d^2 \cdot l}{4}} = \frac{4}{d} \tag{5}$$

To quantify the fiber network density, the fiber length between two conjunctions (unit length) was estimated based on a simplified cubic structure model as described previously [30]. There were three unit fibers in each unit cube. The porosity of the fiber network is given by

$$\varepsilon = 1 - \frac{3V_f}{V_c} \tag{6}$$

where V_f is the volume of one unit fiber and V_c the volume of the unit cube. Substituting Eq. (4) and $V_c = l^3$ into Eq. (6), the porosity is

$$\varepsilon = 1 - \frac{\frac{3\pi \cdot d^2 \cdot l}{4}}{l^3} \tag{7}$$

The unit length is given by rearranging Eq. (7)

$$l = \frac{d}{2}\sqrt{\frac{3\pi}{1 - \varepsilon}} \tag{8}$$

When the fiber diameters were compared, a two-tail Student t-test (assuming equal variances) was performed to determine the statistical significance ($p < 0.05$).

2.3.5. Study on the mechanical properties of the nanoscale fibrous matrices

Uniaxial tensile mechanical testing was performed to evaluate the mechanical properties of the nanofiber matrices using methods similar to those for the mechanical testing of natural and engineered tendon, heart valve, and their scaffolding matrices, with a universal testing instrument (CMT 4204, Sans, China). To measure the mechanical properties of PHA nanofiber matrices, they were prepared in the 120-mm Petri dishes according to the same method used in the 50 mL beaker as described above. They were then cut into strips of approximately $80 \times 10 \times 0.5$ mm^3 for mechanical property testing. A gauge length of 40 mm (distance between two grips) and a crosshead speed of 5 mm/min were used. Six specimens were tested for each sample. The averages and standard deviations from the specimens fractured in the middle (4–6) were reported.

2.3.6. Assays of cell attachment and viability

Studies on the cell attachment and viability were conducted on nanofiber and ordinarily prepared solid-walled matrices using human keratinocyte cell line HaCat, which was purchased from China Center for Type Culture Collection in Wuhan University; 2.0×10^4 cells/well of HaCat was seeded on each matrix measuring

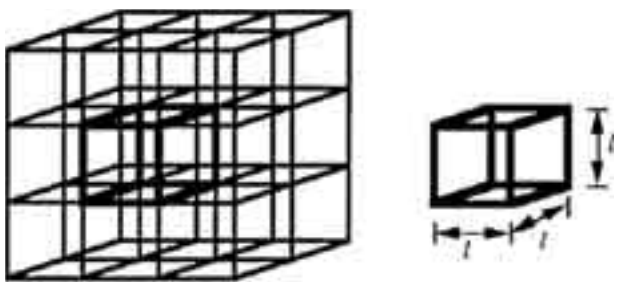

Scheme 1. The model of cubic fiber network.

1.5 cm in diameter placed in the 24-well plates, and cultured in the MEM medium containing 10% FBS.

HaCat cells were incubated at 37 °C for 4 h and 3 days to evaluate cell attachment and viability, respectively. The unattached cells were removed by washing with PBS three times. The number of attached cells was assayed by CCK-8 (Cell Counting Kit-8, Beyotime, China) according to the manufacturers' instructions. The optical density (OD) at 450 nm was determined via a microplate reader (Thermo-Labsystems, Multiskan Mk3, Finland).

3. Results

3.1. Preparation of PHA based nanofiber matrices

To prepare nanoscale matrix, PHB dissolved in chloroform was added with 1,4-dioxane (Diox), tetrahydrofuran (THF) and *N*,*N*-dimethylformamide (DMF), this led to the formation of a PHB gel. Only the addition of Diox turned PHB solution into a nanofiber matrix with diameters ranging from 80 to 350 nm (Fig. 1a and b). DMF and THF created a PHB particle matrix, respectively (Fig. 1c and d). This PHB preparation process differed from that of poly(L-lactide) (PLLA) [30]. The difference can be attributed to the preferred solubility of PHB in chloroform and the proper freezing point of Diox which is at 11.8 °C.

Fabrication of nanofiber matrices made of PHB was studied under different conditions. PHB nanofiber matrix prepared at 4 °C was more homogeneous compared with those prepared under room temperature (23 °C) (Fig. 2a and b). A 1 day water treatment to the PHB gel produced a more satisfactory nanostructure network (Fig. 2a and c). However, ethanol treatment changed the fibrous structures to similar particle matrices (Fig. 2d). In addition, liquid nitrogen or sonication treatment produced more homogeneous nanofibers with diameters of 80–150 nm, especially for sonicated matrices (Fig. 3a–d).

PHB blended with P3HB4HB or PHBHHx was tested for preparation of nanofiber matrices made of various PHAs. At a weight mixing ratio of 70:30 for PHB/PHBHHx or PHB/P3HB4HB, the matrices still showed a continuous fibrous network structure (Fig. 4a and c). While PHB content was lowered to 60% in the blends, the fibrous network structure was diluted significantly compared with pure PHB nanofibers (Fig. 4b and d). It was therefore suggested that the weight mixing ratio of PHB be maintained above 60% in the matrices to allow the formation of a continuous nanoscale fibrous network structure.

The gelation time for forming various nanofiber matrices was studied. It was found that the gelation time decreased with increasing amount of dioxane from 1.0 to 6.0 mL or increasing PHB concentration (Table 1). Gelation temperature affected gelation time; a lower temperature was found more suitable for formation of a high porous nanofiber scaffold (Table 1). Additionally, more PHBHHx or P3HB4HB in the blended matrices could lengthen the gelation time (Table 2).

3.2. Study on main properties of PHA based matrices

The porosity of implant scaffold plays an important role in supporting cell growth in a matrix for tissue regeneration. In this study, the porosities of PHB matrices ranged from 90.1 to 98.4% at 4 °C, and from 85.9 to 95.8% at 23 °C, room temperature (Table 1). Increasing porosity in PHB matrices correlated with increasing amount of Diox in the PHB chloroform solution, up to 98.4% of 6 mL Diox in each 10 mL 1% (wt/v) PHB chloroform solution. In addition, the porosity of nanofiber matrices was influenced by the PHB concentration and gelation temperature to some extend. When PHB was increasingly blended with other PHA materials, the porosities of the nanofiber matrices were also decreased slightly (Table 2). And the blended matrices of PHB/PHBHHx and PHB/P3HB4HB with a ratio of 60/40 had significantly reduced the porosities to 84.4 and 83.8%, respectively (Table 2 and Fig. 4).

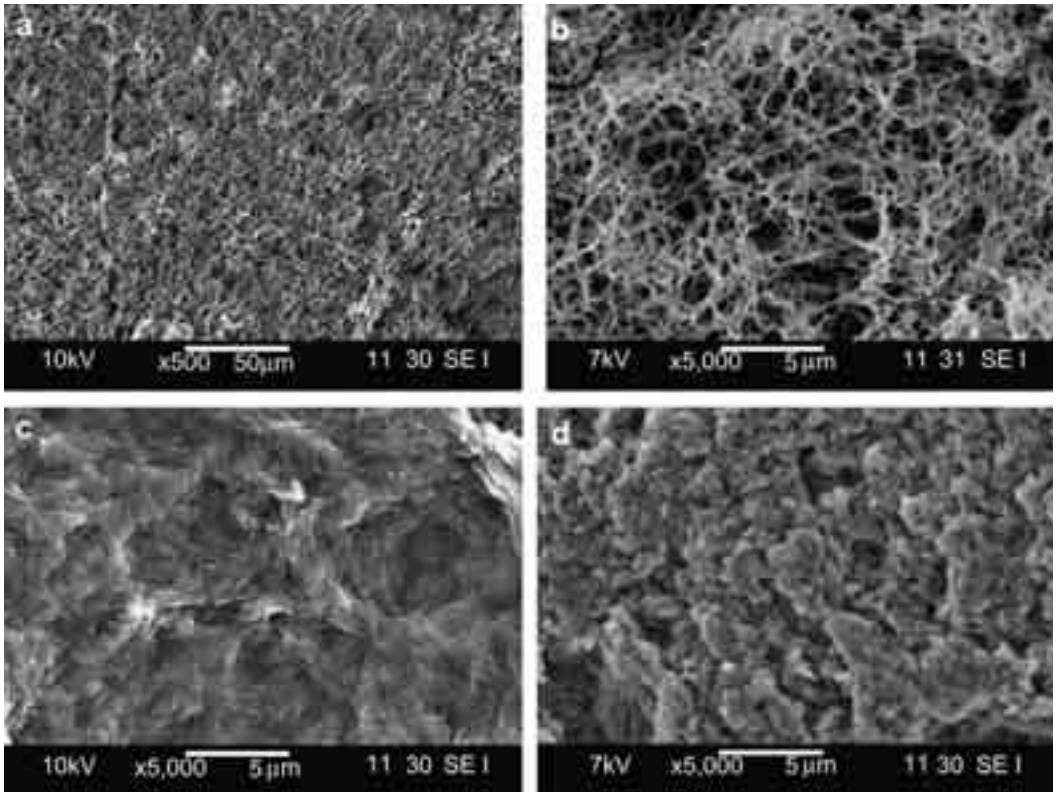

Fig. 1. SEM study of a PHB matrix prepared from 2% (wt/v) PHB chloroform solution at a gelation temperature of 4 °C (a) PHB chloroform/Diox (Dioxane), ×500; (b) PHB chloroform/Diox, ×5000; (c) PHB chloroform/THF (tetrahydrofuran), ×5000; (d) PHB chloroform/DMF (*N*,*N*-dimethylformamide), ×5000.

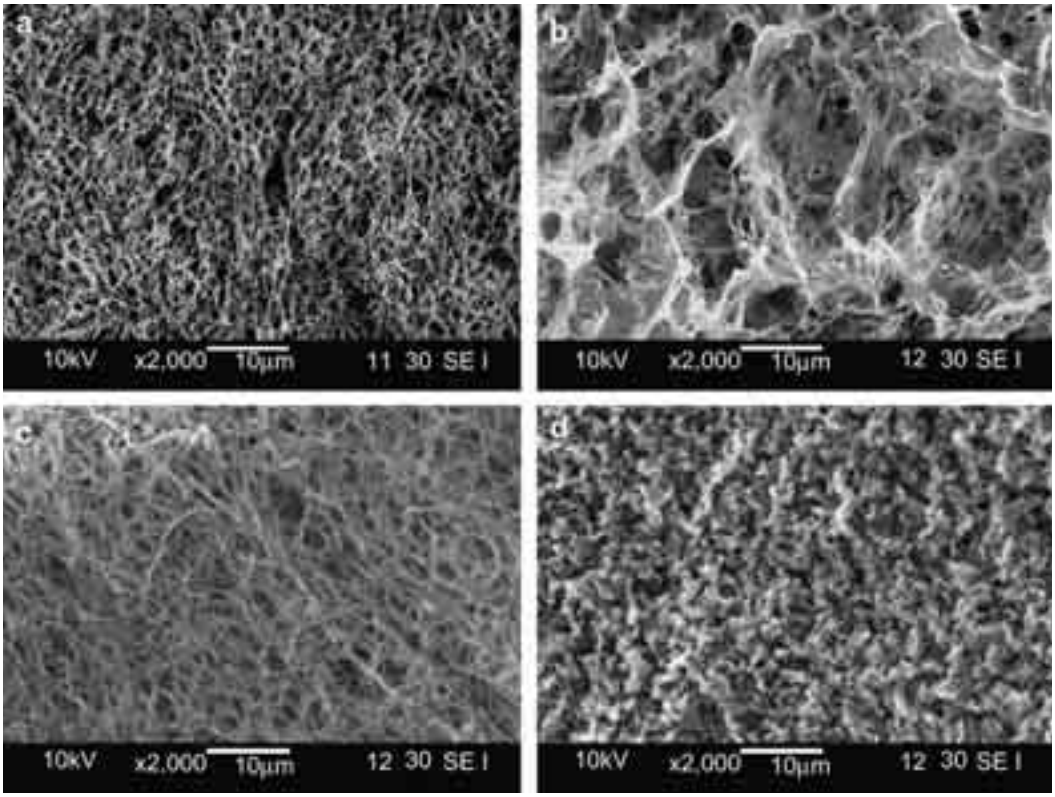

Fig. 2. SEM study of PHB matrices prepared from 2% (wt/v) PHB chloroform solution under various conditions: (a) PHB/control, ×2000; (b) PHB/room temperature (23 °C), ×2000; (c) PHB/without water treatment, ×2000; (d) PHB/with ethanol treatment, ×2000.

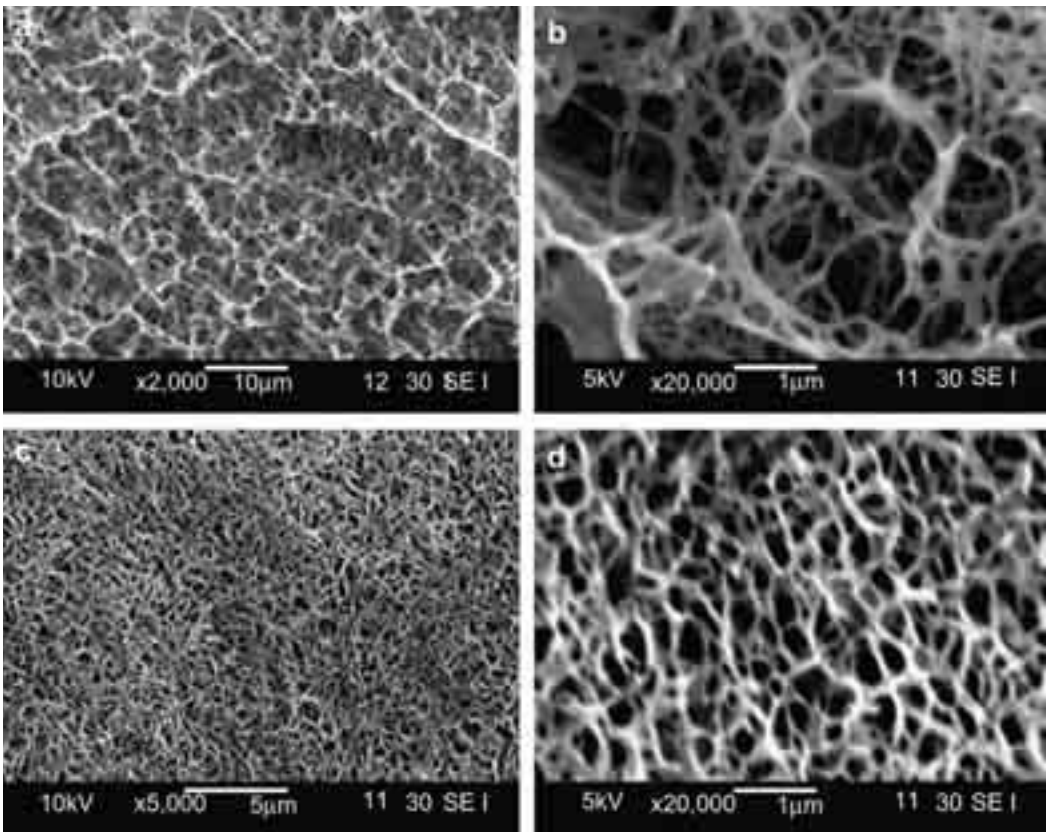

Fig. 3. SEM study of PHB matrices prepared from 2% (wt/v) PHB chloroform solution treated with liquid nitrogen or sonication. PHB matrices treated with liquid nitrogen for 15 min: (a) ×2000; (b) ×20,000. PHB matrices treated with sonication for 20 min: (c) ×5000; (d) ×20,000.

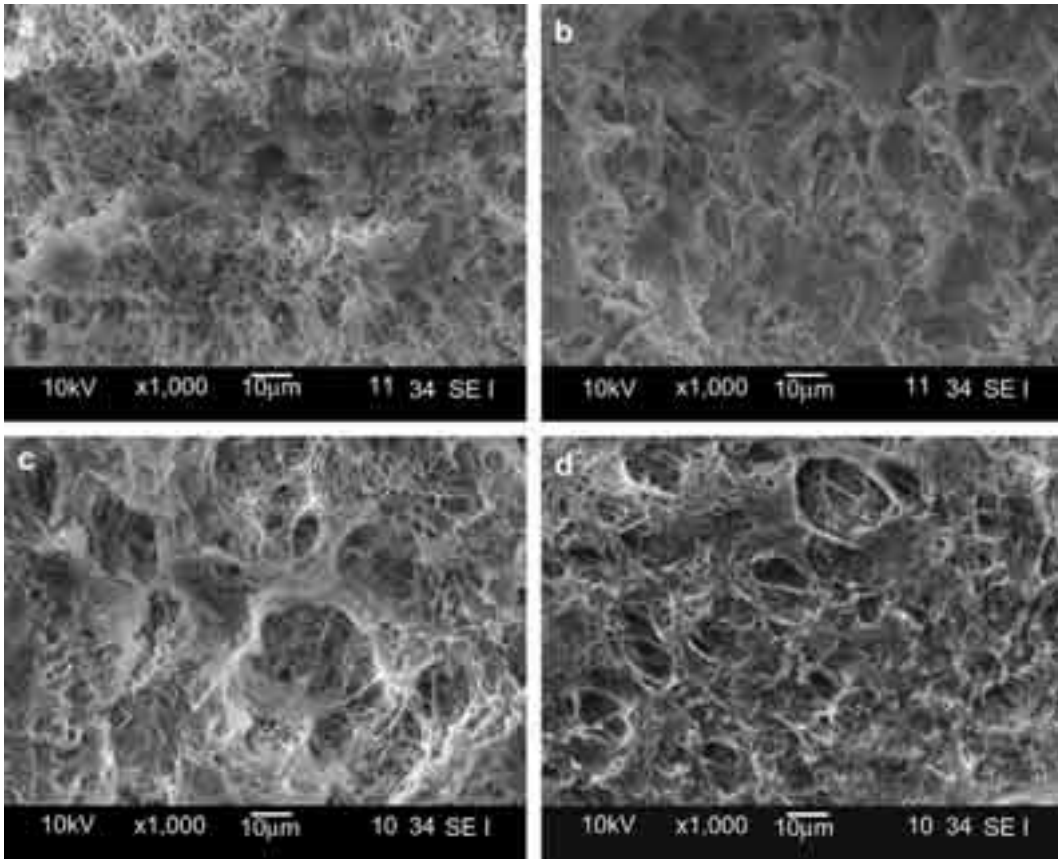

Fig. 4. SEM study of PHA matrices prepared from 2% (wt/v) different PHA blends in the chloroform/dioxane solution: (a) matrix of PHB/PHBHHx = 70:30, ×1000; (b) matrix of PHB/PHBHHx = 60:40, ×1000; (c) matrix of PHB/P3HB4HB = 70:30, ×1000; (d) matrix of PHB/P3HB4HB = 60:40, ×1000.

The nanofiber matrices were composed of continuous fibrous networks with average fiber diameters of approximately 165 ± 80 nm regardless of PHB concentration (Table 3); this result was similar with that of the nanofiber made of PLLA reported by Ma et al. [30]. The surface/volume ratios were also found to be correlated with the average fiber diameters in Eq. (5), ranging from 17.0 to 24.8 μm^{-1} (Table 3). The unit length of PHA matrices related to the porosity and the average fiber diameter in a matrix was described in Eq. (8), this was shown to be 811–1373 nm. The unit length decreased slightly when PHB concentration of the matrix increased (Table 3).

Mechanical properties of nanofiber matrices were significantly improved in the blend matrices made of PHB/PHBHHx or PHB/P3HB4HB (Fig. 5). The modulus, tensile strength and elongation at break showed a significant increase with increasing PHBHHx or P3HB4HB contents in the blended matrices. The mechanical properties of the 60/40 blended PHB/PHA matrices notably increased but diluted the nanofibrous structures (Figs. 4 and 5). However, 70/30 PHB/PHBHHx or PHB/P3HB4HB matrices showed a remarkably improved mechanical strength accompanied by a continuous fibrous network (Figs. 4 and 5).

3.3. Cell behaviors on PHA based matrices

HaCat cells were seeded on the nanofiber matrices and ordinary solid-walled matrices. Cells were found heavily embedded in the PHB nanofiber matrix while they were just adhered on the PHB solid-walled matrix (Fig. 6a and b). Cell attachment and viability were studied using CCK-8 assay according to the manufacturers' instructions. Cell growth was observed to increase remarkably on the nanofiber matrices compared with that in the ordinary solid-walled matrices made of the same materials (Fig. 6c and d). This

Table 1
Gelation behavior and porosity of PHB nanofiber matrices

Concentration of polymer in chloroform		4 °C			23 °C		
		Gelation time (h)	Density (g/mL)	Porosity (%)	Gelation time (h)	Density (g/mL)	Porosity (%)
1% PHB	Diox 1 mL	26.0	0.0862	93.0	19.5	0.1447	88.2
	Diox 2 mL	21.0	0.0648	94.7	19.5	0.1143	90.7
	Diox 3 mL	18.0	0.0455	96.3	19.5	0.0916	92.6
	Diox 4 mL	9.5	0.0351	97.1	14.8	0.0829	93.3
	Diox 5 mL	4.5	0.0307	97.5	8.3	0.0575	95.3
	Diox 6 mL	2.3	0.0203	98.4	5.2	0.0518	95.8
2% PHB/Diox 3 mL		15.0	0.0731	94.6	17.0	0.1138	90.8
3% PHB/Diox 3 mL		8.5	0.1044	91.5	12.5	0.1394	88.7
5% PHB/Diox 3 mL		7.5	0.1217	90.1	10.0	0.1734	85.9

Note that the porosities of PHB matrices were higher at 4 °C than those at 23 °C.

Table 2
Gelation behavior and porosity of various PHA nanofiber matrices obtained at a gelation temperature of 4 °C

Ratio of PHAs	Gelation time (h)	Crystallinity, X_c (%)	Density (g/mL)	Porosity (%)
PHB/PHBHHx 9:1	15.0	64.58	0.0901	92.7
PHB/P3HB4HB 9:1	15.5	63.57	0.0904	92.6
PHB/PHBHHx 8:2	17.5	57.73	0.0844	93.1
PHB/P3HB4HB 8:2	17.5	61.29	0.0932	92.4
PHB/PHBHHx 7:3	18.0	53.75	0.0911	92.5
PHB/P3HB4HB 7:3	18.5	57.86	0.0961	92.1
PHB/PHBHHx 6:4	20.0	50.79	0.1298	84.4
PHB/P3HB4HB 6:4	21.0	53.76	0.1377	83.8

Two percent (wt/v) PHB blended with various weight ratios of PHBHHx or P3HB4HB in the chloroform/dioxane solution.

significant difference was mainly attributed to the nanofiber architecture resembling to that of the natural extracellular matrix [39]. Furthermore, the increase rate with approximately 60% of cell attachment on the PHB nanofiber matrices was most significant compared with that of the other matrices (Fig. 6c), this was mainly attributed to the highest porosity with interconnected porous structure in the PHB nanofiber matrix.

4. Discussion

Polyhydroxyalkanoates (PHAs) especially PHB, PHBV, PHBHHx and P3HB4HB had been strongly demonstrated biodegradability and biocompatibility in vitro and in vivo [1–3]. Many interests have been focused on developing PHA for tissue engineering applications [2,3,14]. However, many of these biomaterials are still different from the real microenvironment of extracellular matrix (ECM); this challenge must be met in order to prepare biomaterials for tissue regeneration [3,17,23]. In our study, a series of nanofiber matrices made of PHA materials were prepared via several unique solution processes. These PHA matrices contain highly porous structures with three-dimensional continuous fibrous networks; such structures are similar to a collagen, which is the most abundant ECM protein in human body [17,34]. At the same time, the average diameter of the PHA nanofibers is similar to the natural collagen fibers, ranging from 50 to 500 nm [24,25].

The nanofibrous structure of PHB matrix was formed when Diox was added into the PHB chloroform solution, other non-solvents such as THF and DMF could not produce the nanofibrous structures (Fig. 1). The process differs from the preparation of PLLA nanofibrous matrices, and mainly dues to the different solubility of PHB and PLLA [30,33]. The gel formed at 4 °C and treated with water within a day produced satisfactory nanofibrous structures (Fig. 2), especially with the additional treatment of liquid nitrogen or sonication before gelation, respectively (Fig. 3). The treatment using liquid nitrogen or sonication led to a more homogeneous

Table 3
Structural parameters of nanofibrous matrices prepared from various PHAs in chloroform/dioxane at 4 °C

Concentration and ratios of PHA	Diameter (nm)	Unit length (nm)	Surface/volume ratio (μm^{-1})
PHB 1%	161 ± 84	1285	24.8
PHB 2%	166 ± 80	909	24.1
PHB 3%	170 ± 75	895	23.5
PHB 5%	167 ± 91	811	24.0
PHB/PHBHHx 9:1	210 ± 77	1191	19.0
PHB/P3HB4HB 9:1	198 ± 90	1120	20.2
PHB/PHBHHx 8:2	235 ± 83	1373	17.0
PHB/P3HB4HB 8:2	225 ± 81	1253	17.8
PHB/PHBHHx 7:3	220 ± 94	1236	18.2
PHB/P3HB4HB 7:3	224 ± 76	1227	17.9

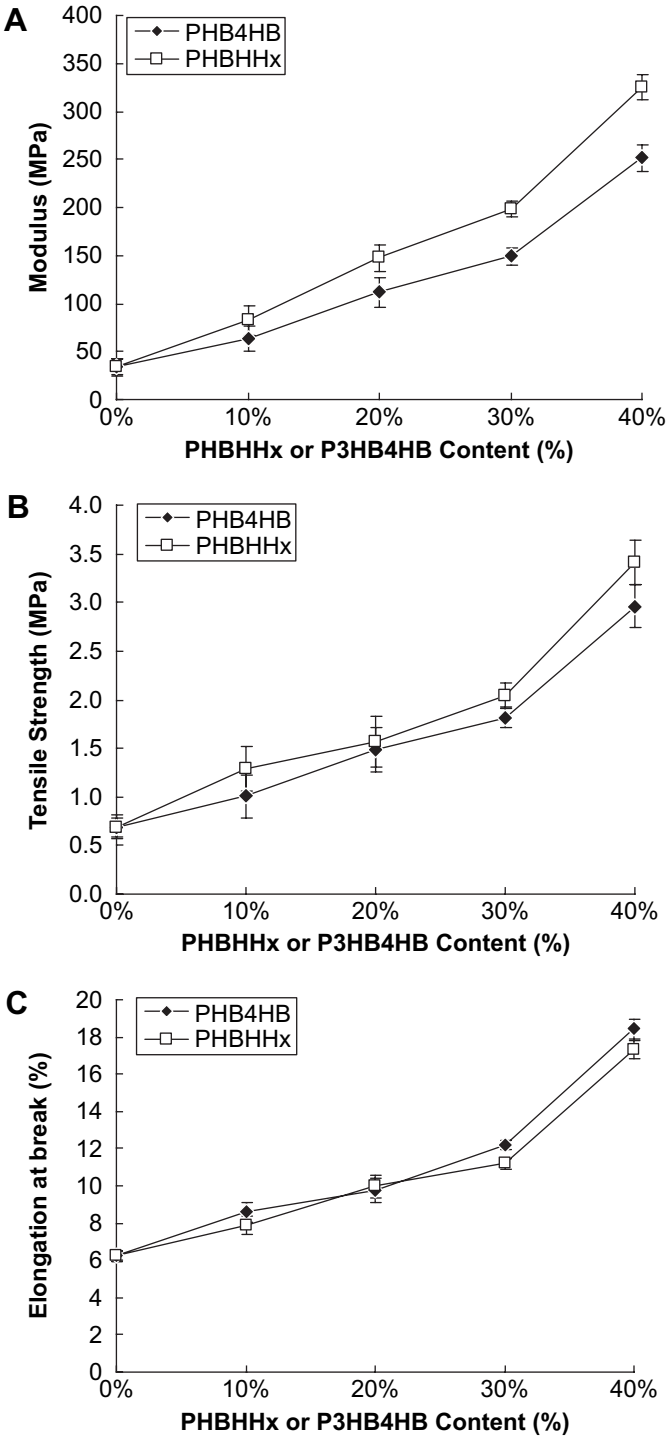

Fig. 5. Mechanical properties of various PHA nanofiber matrices prepared from 2% (wt/v) chloroform/dioxane at a gelation temperature of 4 °C: (a) modulus of PHB/PHBHHx or PHB/P3HB4HB nanofiber matrices in various ratios. (b) Tensile strength of PHB/PHBHHx or PHB/P3HB4HB nanofiber matrices in various ratios. (c) Elongation at break of PHB/PHBHHx or PHB/P3HB4HB nanofiber matrices in various ratios.

nanostructure with fiber diameters ranging from 80 to 150 nm (Fig. 3b and d), Unfortunately, the mechanical strengths through both treatments became too brittle to determine by instrument. Other lower temperatures such as −20 or −80 °C had little influence on the formation of PHA nanofiber matrix, which is similar to the preparation process for PLLA nanofiber [30]. Our results revealed that the gelation time depended on PHB concentration and the amount of Diox added to the PHB solution (Table 1). With

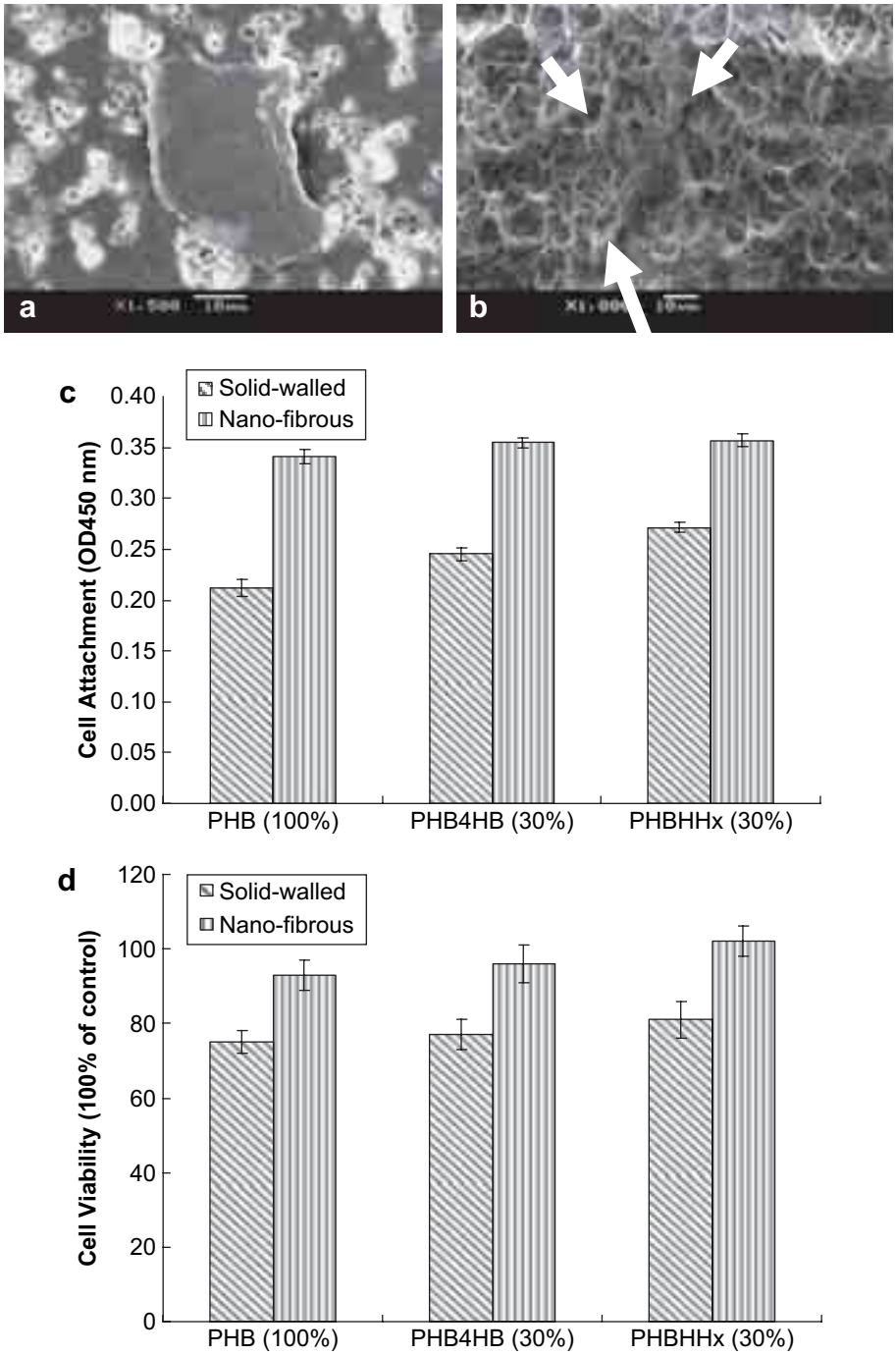

Fig. 6. Cell behavior of HaCat on the solid-walled and nanofibrous matrices made of PHB, PHB/PHBHHx (70:30) and PHB/P3HB4HB (70:30). (a) SEM image of HaCat cell on the PHB solid-walled matrix; (b) SEM image of HaCat cell on the PHB nanofibrous matrix. Arrows indicate the spreading of the cell. Cell growth was assayed by CCK-8 (Cell Counting Kit-8) at a wavelength of 450 nm ($n = 6$): (c) 2.0×10^4 cells/well were seeded on each matrix placed in the 24-well plates to valuate cell attachment for 4 h, the wells with only culture medium were used as blank. (d) 2.0×10^4 cells/well were seeded on each matrix placed in the 24-well plates to valuate cell viability for 3 days, the wells in which only cells were seeded without the matrices were used as 100% control.

Diox concentration over 3.0 mL in 10 mL PHB solution, the gelation time was shortened significantly (Table 1). Obviously the PHA gelation behavior is influenced by both quantity of the PHA non-solvent Diox and solvent chloroform, a PHA solution could become a gel when Diox and chloroform were mixed in a proper ratio. More Diox in PHA solution was beneficial for forming a nanofibrous continuous network with high porosity (Table 1). However, when the amount of Diox was added over 4.0 mL into 10 mL 1% PHB solution, the matrix was stuck on the beaker so that the mechanical strength can't be evaluated. After a series optimization, following conditions including 3.0 mL Diox in 10 mL PHA solution and a gelation temperature of 4 °C for a 15–21 h followed by 24 h water treatment were selected for PHA nanofibrous matrix preparation.

Our technique belongs to a phase separation of polymer solution, which can also be considered a self-assembly process. Instead of assembling small molecules, large molecules of polymer are aggregated into a new phase from an initially homogeneous one-phase system [21]. Compared with conventional electrospun process for making nanofiber [40], our technique for preparing the PHA nanofiber matrices is simple; it does not require any expensive

equipment and complicated processing. Moreover, the architecture from electrospinning is often lacked of a natural three-dimensional morphology that is through self-assembled behaviors [21,29]. Therefore, our technique is very helpful for developing novel nanostructure implant PHA matrices for applications in tissue engineering.

A highly porous structure with interconnected spaces is desirable for an implant scaffold as this structure will provide ECM mimic base for cell attachment, migration and proliferation [23,35]. Increasing the amount of Diox in the PHB chloroform solution can increase the porosity of PHB matrix, up to 98.4% of 6 mL Diox in each 10 mL 1% (wt/v) PHB chloroform solution, but reduces the mechanical strength to some extend. These matrices of PHB/PHBHHx or PHB/P3HB4HB showed decreased porosities from 94.6% for PHB only matrices (Table 1) to 83.8–93.1% for the blended matrices (Table 2) accompanied with reduced crystallinity and blurred nanofibrous structure when PHB content in the blends decreased (Table 2 and Fig. 4). At the highest ratio of 60/40 for PHB/PHBHHx or PHB/P3HB4HB, gelation time was over 20 h, the longest among all blended samples studied, the blends showed the lowest crystallinity and the smallest porosity yet the highest density (Table 2), accompanied by the best mechanical properties (Fig. 5). This phenomenon was mainly attributed to the amorphous part of PHBHHx or P3HB4HB in the blends that reduced the crystallinity of highly crystal PHB [38], thus contributes to improve the weak properties of crystal PHB [15,16]. However, reduced crystallinity of a polymer prevented the formation of a clear nanofibrous structure [30]. As a compromise, it was found that 70/30 PHB/PHBHHx or PHB/P3HB4HB matrix showed a combination of improved mechanical strength and formation of a clear continuous nanofiber network (Figs. 4 and 5). To prepare such an ECM mimic structure, a proper surface-to-volume ratio is required [36]. Apparently, PHB only matrices showed higher surface-to-volume ratios compared with the PHA blends, and a higher PHB content in the PHA blends led to a higher surface-to-volume ratios (Table 3). All the PHA nanofibrous structures supported better cell growth compared with PHA solid-walled films without the highly porous nanostructure (Fig. 6).

Besides the cell growth supporting ability, mechanical properties of a polymer matrix are important for selection of biomaterials in tissue engineering; especially for application in a load-bearing position such as bone fixation, replacement or artificial blood vessels [35,37]. The presence of elastic PHBHHx or P3HB4HB in the PHB dominated blended matrices increased their modulus, tensile strength and elongation at break (Fig. 5). In this study, mechanical properties of 60/40 PHB/PHA blended matrices showed maxima due to their completed miscibility and reduced polymer crystallinity [15,16]; but the nanofibrous structures were diluted notably (Fig. 4b and d). In contrast, Young's modulus, tensile strength and elongation at break of 70/30 PHB/PHA nanofiber matrix were approximately 150 MPa, 1.8 MPa and 11.5%, respectively, accompanied by a still continuous fibrous nanostructure (Fig. 4a and c). As expected, the fiber diameter and fiber unit length could influence the mechanical properties of the matrix to some extent (Table 3 and Fig. 5). Thus, the PHA nanofiber matrices indicated significantly improved mechanical properties with proper adjustability advantages over other nanofiber matrices, such as PLLA nanofiber matrix reported by Ma et al. [17,30]. Young's modulus, tensile strength and elongation at break of 2% (wt/v) PLLA nanofiber matrix are 4.0 MPa, 0.1 MPa and 6.1%, respectively [30], which are all inferior to that of PHA nanofiber matrices, especially the blended PHA nanofiber matrix in a proper ratio.

HaCat cells' growth on matrices made of PHB, PHB/PHBHHx (70:30) or PHB/P3HB4HB (70:30) was assayed to evaluate the effect of nanofiber matrix. Results strongly demonstrated that cell behaviors including morphology, adhesion ability and viability on the nanofibrous matrices were better than those on the ordinary solid-walled matrices (Fig. 6). The nanofiber architecture resembling the collagen as a main component of the natural extracellular matrix could play a key role for better cell attachment, migration, growth and function in tissue regeneration [34]. The influences of nanoscale structures on cell behaviors were reported as early as 1960s [41], cells were found attached to and organized around fibers with diameters smaller than that of the cells [42]. Some scaffolds made of PLA, PLGA and PHA contain often microfibers with diameter of 5–50 μm or micropores of 10–50 μm [3,43]. Since the size of most cells (5–10 μm) is similar to or smaller than these microstructures (10–100 μm), these cells exhibit a two-dimensional topography with a curvature depending on the microfiber diameters or on the pore size upon their attachment [23]. In order to culture cells in a truly three-dimensional microenvironment, these dimensions must be significantly smaller than cells so that the cells could be surrounded by the scaffolds, much like the extracellular environment [23]. Thus, the nanofibrous matrix such as PHA nanofiber matrix is a real three-dimensional microenvironment for cells [43]. Our results of PHA nanofibers were consistent with some recent investigations using nanostructural materials as artificial ECM [44–46].

5. Conclusions

We had successfully fabricated PHB, PHB/PHBHHx and PHB/P3HB4HB nanofiber matrices that combine the advantages of biodegradability, biocompatibility, improved mechanical strength and similarity to architectures of natural collagen extracellular matrix. These PHA nanofiber matrices were found to better support cell attachment and cell viability compared with PHA solid-walled matrices prepared from ordinary solution casting method. Mechanical properties, porosity and nanostructure of the matrices can be adjusted by changing PHB to PHBHHx or to P3HB4HB ratios in the blend. Compared with conventional electrospun process for making nanofiber, our technique for preparing the PHA nanofiber matrices is simple; it does not require any equipment and complicated processing such as fiber extrusion, drawing, crimping, cutting, carding, needling, degreasing and punching. This is very helpful for developing novel nanostructure implant PHA matrices for applications in skin engineering and even nerve regeneration [47,48]. The future studies will be performed for practical applications in vitro and in vivo.

Acknowledgments

The research was supported by Li Ka Sheng Foundation and National High Tech 863 Grant (Project No. 2006AA02Z242), as well as the State Basic Science Foundation 973 (2007CB707804). Guangdong Provincial Grant for collaboration among industry, university and research organization awarded to GQC has initiated this study. We thank Lin Yuejuan in the Analysis Center of Shantou University for assistance in many SEM studies.

References

[1] Hazer B, Steinbüchel A. Increased diversification of polyhydroxyalkanoates by modification reactions for industrial and medical applications. Appl Microbiol Biotechnol 2007;74:1–12.
[2] Valappil SP, Misra SK, Boccaccini AR, Roy I. Biomedical applications of polyhydroxyalkanoates: an overview of animal testing and in vivo responses. Expert Rev Med Devices 2006;3:853–68.
[3] Chen GQ, Wu Q. Polyhydroxyalkanoates as tissue engineering materials. Biomaterials 2005;26:6565–78.
[4] Tian G, Wu Q, Sun SQ, Noda I, Chen GQ. Study of thermal melting behavior of microbial polyhydroxyalkanoates using two-dimensional Fourier-transform infrared FT-IR correlation spectroscopy. Appl Spectrosc 2001;55:888–94.
[5] Miller ND, Williams DF. On the biodegradation of poly-beta-hydroxybutyrate homopolymer and poly beta-hydroxybutyrate–hydroxyvalerate copolymers. Biomaterials 1987;8:129–37.

[6] Shishatskaya EI, Volova TG, Puzyr AP, Mogilnaya OA, Efremov SN. Tissue response to the implantation of biodegradable polyhydroxyalkanoate sutures. J Mater Sci Mater Med 2004;15:719–28.
[7] Mosahebi A, Fuller P, Wiberg M, Terenghi G. Effect of allogeneic Schwann cell transplantation on peripheral nerve regeneration. Exp Neurol 2002;173:213–23.
[8] Williams SF, Martin DP. Application of PHAs in medicine and pharmacy. In: Doi Y, Steinbüchel A, editors. Biopolymers, vol. 10. Weinheim: Wiley-VCH; 2002. p. 91–121.
[9] Freier T, Kunze C, Nischan C, Kramer S, Sternberg K, Saß M, et al. In vitro and in vivo degradation studies for development of a biodegradable patch based on poly(3-hydroxybutyrate). Biomaterials 2002;23:2649–57.
[10] Barham PJ, Keller A. The relationship between microstructure and mode of fracture in polyhydroxybutyrate. J Polym Sci Part B Polym Phys 1986;24:69–77.
[11] Kenong GJ, Lemstra PJ. Crystallization phenomena in bacterial poly(3-hydroxybutyrate): 2. Embrittlement and rejuvenation. Polymer 1993;34:4089–94.
[12] Xu J, Guo BH, Chen GQ, Zhang ZM. Terraces on banded spherulites of polyhydroxyalkanoates. J Polym Sci Part B Polym Phys 2003;41:2128–34.
[13] Chen GQ, Wu Q, Zhao K, Yu HP, Chan A. Chiral biopolyesters–polyhydroxyalkanoates synthesized by microorganisms. Chin J Polym Sci 2000;18:389–96.
[14] Misra SK, Valappil SP, Roy I, Boccaccini AR. Polyhydroxyalkanoate (PHA)/inorganic phase composites for tissue engineering applications. Biomacromolecules 2006;7:2249–58.
[15] Zheng Z, Bei FF, Deng Y, Tian HL, Chen GQ. Effects of crystallization of polyhydroxyalkanoate blend on surface physicochemical properties and resulting biocompatibility for chondrocytes. Biomaterials 2005;26:3537–48.
[16] Luo RC, Xu KT, Chen GQ. Study of miscibility, crystallization, mechanical properties, and thermal stability of blends of poly(3-hydroxybutyrate) and poly(3-hydroxybutyrate-*co*-4-hydroxybutyrate). J Appl Polym Sci 2007;105:3402–8.
[17] Ma PX. Biomimetic materials for tissue engineering. Adv Drug Deliv Rev 2008;60:184–98.
[18] Lu LC, Peter SJ, Lyman MD, Lai HL, Leite SM, Tamad JA, et al. In vitro degradation of porous poly(L-lactic acid) foams. Biomaterials 2000;21:1595–605.
[19] Niklason LE, Gao J, Abbott WM, Hirschi KK, Houser S, Marini R, et al. Functional arteries grown in vitro. Science 1999;284:489–93.
[20] Ma PX, Zhang R. Microtubular architecture of biodegradable polymer scaffolds. J Biomed Mater Res 2001;56:469–77.
[21] Ma PX. Scaffolds for tissue fabrication. Mater Today 2004;7:30–40.
[22] Hartgerink JD, Beniash E, Stupp SI. Self-assembly and mineralization of peptide–amphiphile nanofibers. Science 2001;294:1684–8.
[23] Gelain F, Horii A, Zhang SG. Designer self-assembling peptide scaffolds for 3-D tissue cell cultures and regenerative medicine. Macromol Biosci 2007;7:544–51.
[24] Elsdale T, Bard J. Collagen substrata for studies on cell behavior. J Cell Biol 1972;54:626–37.
[25] Hay ED. In: Hay ED, editor. Cell biology of extracellular matrix. 2nd ed. New York: Plenum Press; 1991. p. 56–7.
[26] Holmes TC, Lacalle S, Su X, Liu G, Rich A, Zhang SG. Extensive neurite outgrowth and active synapse formation on self-assembling peptide scaffolds. Proc Natl Acad Sci U S A 2000;97:6728–33.
[27] Horii A, Wang X, Gelain F, Zhang SG. Biological designer self-assembling peptide nanofiber scaffolds significantly enhance osteoblast proliferation, differentiation and 3-D migration. PLoS ONE 2007;2(2):e190. doi:10.1371/journal.pone.0000190.
[28] Gelain F, Bottai D, Vescovi A, Zhang SG. Designer self-assembling peptide nanofiber scaffolds for adult mouse neural stem cell 3-dimensional cultures. PLoS ONE 2006;1(1):e119. doi:10.1371/journal.pone.0000119.
[29] Zhang SG. Fabrication of novel biomaterials through molecular self-assembly. Nat Biotechnol 2003;21:1171–8.
[30] Ma PX, Zhang R. Synthetic nano-scale fibrous extracellular matrix. J Biomed Mater Res 1999;46:60–72.
[31] Chen VJ, Smith LA, Ma PX. Bone regeneration on computer-designed nanofibrous scaffolds. Biomaterials 2006;27:3973–9.
[32] Vonk CG. Computerization of Ruland's X-ray method for determination of the crystallinity in polymers. J Appl Crystallogr 1973;6:148–52.
[33] Barham PJ, Keller A, Otun EL, Holmes PA. Crystallization and morphology of a bacterial thermoplastic: poly-3-hydroxybutyrate. J Mater Sci 1984;19:2781–94.
[34] Grinnell F, Bennett MH. Ultrastructural studies of cell–collagen interactions. Methods Enzymol 1982;82:535–44.
[35] Shin M, Abukawa H, Troulis M, Vacanti JP. Development of a biodegradable scaffold with interconnected pores by heat fusion and its application to bone tissue engineering. J Biomed Mater Res 2008;84A:702–9.
[36] Mikos AG, Thorsen AJ, Czerwonka LA, Bao Y, Langer R, Winslow DN, et al. Preparation and characterization of poly(L-lactic acid) foams. Polymer 1994;5:1068–77.
[37] Chiu JB, Liu C, Hsiao BS, Chu B, Hadjiargyrou M. Functionalization of poly(L-lactide) nanofibrous scaffolds with bioactive collagen molecules. J Biomed Mater Res 2007;83A:1117–27.
[38] Qu XH, Wu Q, Liang J, Zou B, Chen GQ. Effect of 3-hydroxyhexanoate content in poly(3-hydroxybutyrate-*co*-3-hydroxyhexanoate) on in vitro growth and differentiation of smooth muscle cells. Biomaterials 2006;27:2944–50.
[39] Woo KM, Chen VJ, Ma PX. Nano-fibrous scaffolding architecture selectively enhances protein adsorption contributing to cell attachment. J Biomed Mater Res 2003;67A:531–7.
[40] Ma ZW, Kotaki M, Inai R, Ramakrishna S. Potential of nanofiber matrix as tissue-engineering scaffolds. Tissue Eng 2005;11:101–9.
[41] Rosenberg MD. Cell guidance by alterations in monomolecular films. Science 1963;139:411–2.
[42] Laurencin CT, Ambrosio AMA, Borden MD, Cooper JJ. Tissue engineering: orthopedic applications. Annu Rev Biomed Eng 1999;1:19–46.
[43] Zhang S. Beyond the Petri dish. Nat Biotechnol 2004;22:151–2.
[44] Tian F, Hosseinkhani H, Hosseinkhani M, Khademhosseini A, Yokoyama Y, Estrada GG, et al. Quantitative analysis of cell adhesion on aligned micro- and nanofibers. J Biomed Mater Res 2008;84A:291–9.
[45] Woo KM, Jun JH, Chen VJ, Seo J, Baek JH, Ryoo HM, et al. Nano-fibrous scaffolding promotes osteoblast differentiation and biomineralization. Biomaterials 2007;28:335–43.
[46] Ellis-Behnke RG, Liang YX, You SW, Tay DKC, Zhang SG, So KF, et al. Nano neuro knitting: peptide nanofiber scaffold for brain repair and axon regeneration with functional return of vision. Proc Natl Acad Sci U S A 2006;103:5054–9.
[47] MacNeil S. Progress and opportunities for tissue-engineered skin. Nature 2007;445:874–80.
[48] Schmidt CE, Leach JB. Neural tissue engineering: strategies for repair and regeneration. Annu Rev Biomed Eng 2003;5:293–347.